1

Validation of the Geostationary Lightning Mapper with a
Lightning Mapping Array in Argentina:
Implications for Current and Future Spaceborne Lightning Observations

5
6

Timothy J. Lang[1]

[1]NASA Marshall Space Flight Center, Huntsville, Alabama.

9
10

Corresponding author: Timothy Lang (timothy.j.lang@nasa.gov)

12
13

Key Points:

- The Geostationary Lightning Mapper detected lightning with overall 75% efficiency relative to a ground network in Argentina.
- Detection efficiency depended significantly on day/night, and on flash rate, size, altitude, and the presence of anomalous lightning.
- An improved sensor that could better detect and distinguish between small flashes would provide more information about storm evolution.

Abstract

A validation study of the Geostationary Lightning Mapper (GLM) on board the Geostationary Operational Environmental Satellite 16 (GOES-16) was done using a ground-based lightning mapping array (LMA) deployed as part of the Remote sensing of Electrification, Lightning, And Mesoscale/microscale Processes with Adaptive Ground Observations (RELAMPAGO) field campaign in Argentina. GLM detected lightning with 74.6% efficiency over 61 thunderstorm days in December 2018 through April 2019. However, GLM detection efficiency (DE) was negatively correlated ($r = -0.49$) with LMA flash rate. GLM DE also was negatively correlated with LMA flash altitude ($r = -0.24$), reflecting the influence of multiple competing trends. GLM DE was positively correlated ($r = 0.27$) with number of LMA sources in a flash, indicating improved DE for larger flashes. During periods with anomalously electrified storms, GLM DE was reduced to 50.9%. Statistics were found to be sensitive to analysis criteria, but most of the above trends remained consistent regardless of specific criteria. Because the methodology allowed a GLM flash to match more than one LMA flash, actual GLM flash rate was a factor of 2.9 lower than the LMA flash rate, and this ratio grew larger as LMA flash rate increased. A sensitivity study examined the impact of improved DE for smaller flashes; that is, an improved sensor (or algorithm) that was better able to detect and distinguish between separate small lightning flashes. The results showed improved correlation with LMA flash rates, as well as improved ability to identify lightning jumps associated with intensifying convection.

Plain Language Summary

Based on a comparison with a ground-based, three-dimensional lightning detection system in Argentina, the Geostationary Lightning Mapper (GLM) on board the Geostationary Operational Environmental Satellite 16 (GOES-16) detects lightning with nearly 75% efficiency, which meets its requirements. However, that detection efficiency decreases a lot when thunderstorms produce a lot of lightning at once, or small lightning flashes, or when lightning occurs deeper in the cloud where it is more difficult for the optical pulse to make its way to cloud top. This makes GLM somewhat less useful during the most intense part of a storm's life. However, if GLM or a similar sensor could be made more sensitive, either with improved hardware design or better data processing, then it would become more useful in intense storms.

1 Introduction

Ever since the Geostationary Lightning Mapper (GLM) on board the Geostationary Operational Environmental Satellite 16 (GOES-16) first began operating in 2017, it has been recognized as a highly successful instrument that makes critical and continuous observations of lightning across its quasi-hemispheric field of view (Rudlosky et al. 2019). Since then, two additional GLMs – on GOES-17 and -18 – have launched (e.g., Bateman et al. 2021, Rudlosky & Virts 2021). Due to its continuous monitoring capability, GLM regularly observes far more lightning than its predecessors. For example, the Lightning Imaging Sensor (LIS), which has been hosted on the Tropical Rainfall Measuring Mission (TRMM; Kummerow et al. 1998) and the International Space Station (ISS; Blakeslee et al. 2020), provided much of the design heritage for GLM (in particular, the focus on the 777.4-nm oxygen triplet, which enables optical detection of lightning during daytime; Goodman et al. 2013), but due to its low-Earth orbit (LEO) cannot

67 observe in raw numbers as much lightning as GLM. LIS, along with its predecessor the Optical
68 Transient Detector (OTD; Christian et al. 2003), has been aimed at documenting global
69 lightning, which GLM cannot do.
70   However, because it views continuously and observes so much lightning, issues have
71 been noted with GLM that were not as well-documented with previous spaceborne lightning
72 mappers, despite the common design heritage. One major area of concern has been false alarms;
73 that is, event detections that do not correspond to actual lightning (Bateman & Mach 2020,
74 Peterson 2020, Bateman et al. 2021). These often manifest as solar glint (either off clouds or
75 reflective surfaces like water), or artifacts manifested by GLM electronics (e.g., "Bahama bars";
76 Bateman & Mach 2020). However, though they are challenging to address in processing
77 algorithms, it is relatively straightforward to document these issues, as reference ground- and
78 space-based datasets exist for cross-check (though challenges still remain; Virts & Koshak
79 2023). Moreover, false alarms often are dependent on relatively predictable patterns (e.g., solar
80 reflections as the sun moves across the GLM field of view). Also, false alarms don't seem to be
81 as large of a concern in LEO missions like LIS (Blakeslee et al. 2020, Lang & Bang 2022).
82   Perhaps more concerning, then, is the lightning that GLM (and by extension, other
83 missions that use the 777.4 nm detection capability) may miss. GLM was designed to provide
84 70% minimum detection efficiency (DE) averaged across the field of view (Goodman et al.
85 2013). This is likely as good or better than what TRMM LIS was able to provide, and is better
86 than the ~60% DE provided by ISS LIS (Blakeslee et al. 2020). But not all lightning is created
87 equal, and GLM (and related missions') DE may be a strong function of lightning type and
88 thunderstorm evolutionary state (Murphy & Said 2020, Rutledge et al. 2020, Zhang & Cummins
89 2020, Peterson 2021a).
90   One of the critical services that GLM provides is continuous monitoring of severe storms.
91 A notable feature of severe storms is their propensity to produce a lot of lightning flashes,
92 particularly while intensifying prior to the production of strong winds, hail, or tornadoes. This
93 so-called "lightning jump" (Williams et al. 1999, Schultz et al. 2009, Gatlin & Goodman 2010,
94 Chronis et al. 2015) was originally identified using three-dimensional total lightning mappers
95 that detect close to 100% of the lightning within their range (~100 km). The lightning jump is
96 clearly linked to significant kinematic and microphysical changes in thunderstorms as they
97 evolve (Chronis et al. 2015, Schultz et al. 2015, 2017). One change that is very common is
98 increased updraft strength, which leads to increased frequency of small-scale turbulent eddies
99 that separate charge over smaller distances, subsequently encouraging smaller flashes near
100 updrafts compared to further away (Bruning & MacGorman 2013, Schultz et al. 2015).
101   To summarize, then, intense or severe thunderstorms are highly likely to produce a lot of
102 small lightning flashes near their updraft cores. However, these flashes are also the kind of
103 lightning that GLM is most likely to miss. This is because the flashes may produce a reduced
104 amount of optical energy, and they may fall below the horizontal spatial resolution of GLM (~8-
105 10 km). And due to the design heritage, there is no reason to think that similar instruments like
106 LIS would not be similarly challenged (Zhang & Cummins 2020).
107   An additional issue is anomalous storms; that is, storms that tend to have a preponderance
108 of positive electrical charge at mid-levels (roughly -10 to -20 °C) compared to typical storms
109 (Rust et al. 2005; Wiens et al. 2005; Bruning et al. 2014). A major consequence of this is most of
110 the lightning in these storms occurs lower in altitude within the cloud. This naturally limits the
111 amount of optical scattering reaching cloud top, upon which imagers like GLM, LIS, etc. depend
112 (Marchand et al. 2019, Rutledge et al. 2020, Peterson et al. 2021).

113   Thus, the focus of this study will be on quantitatively documenting how GLM-16 DE
114   evolves as lightning and thunderstorms evolve. This will enable us to understand how to properly
115   interpret GLM (and similar) observations when DE is expected to be challenged (e.g., small
116   flashes in severe storms, anomalous storms, etc.). The domain of interest is a three-dimensional
117   (3D) lightning mapping network in north-central Argentina, which was deployed in support of
118   the Remote sensing of Electrification, Lightning, And Mesoscale/microscale Processes with
119   Adaptive Ground Observations (RELAMPAGO) field campaign (Nesbitt et al. 2021). GLM
120   performance in this domain was studied by Lang et al. (2020); however, that study only
121   examined two cases. The present study will build on this to examine a multi-month period,
122   enabling a high level of statistical confidence in the results. Argentina is an excellent domain to
123   study because severe weather is relatively common there (Nesbitt et al. 2021), and anomalous
124   storms also can occur (Medina et al. 2022).
125   While this study will focus on GLM-16, its results will be relevant to similar missions.
126   This includes current geostationary instruments like GLM-17/18, Lightning Mapping Imager
127   (LMI; Cao et al. 2021), and Meteosat Third Generation Lightning Imager (MTG-LI; Holmlund
128   et al. 2021). It also includes LEO missions like LIS (both TRMM and ISS), OTD, Fast On-orbit
129   Recording of Transient Events (FORTE; Suszcynsky et al. 2001), and the Atmosphere-Space
130   Interactions Monitor (ASIM; Neubert et al. 2019). Ultimately, any instrument focused on
131   measuring lightning via the 777.4-nm optical emission band is going to be affected by day/night
132   asymmetries in DE, as well as challenges in detecting small, optically dim flashes, or lightning
133   occurring within optically thick clouds.
134   It should be noted that ASIM also monitors lightning at 337 nm (Chanrion et al. 2019).
135   This ultraviolet (UV) band is typically more sensitive to colder streamer activity, compared to
136   777.4 nm which is more sensitive to hotter leader activity. Indeed, there appears to be a
137   population of lightning flashes that are predominantly more detectable at 337 vs. 777 nm (Soler
138   et al. 2021). Similarly, there are flashes that are more readily detectable in radio frequency (RF)
139   compared to optical frequencies (e.g., Jacobson & Light 2012). These flash detectability
140   differences have important implications for single-channel sensors like GLM, LIS, etc.
141   Specifically, a multi-frequency approach may yield important detectability improvements that
142   allow overall a more representative population of lightning flashes to be detected. This could
143   have benefits for algorithms based on phenomena like lightning jumps. Thus, it would be helpful
144   to understand what benefits may accrue based on improved DE of additional lightning flashes.
145
146   **2 Data and Methods**
147
148   2.1 Geostationary Lightning Mapper (GLM)
149
150   For this study, the GLM on GOES-16 was used. This sensor has already undergone a
151   validation process (e.g., Bateman & Mach 2020, Quick et al. 2020, Virts & Koshak 2020) by the
152   National Aeronautics and Space Administration (NASA) and the National Oceanic and
153   Atmospheric Administration (NOAA); however, it remains useful to continue probing potential
154   limitations of the instrument, so that its full scientific potential can be understood. This study
155   used the Level 2 datasets provided by the Lightning Cluster Flash Algorithm (LCFA; GOES-R
156   2018), which identifies Flashes as a collection of Groups, and Groups as a collection of Events
157   (Mach 2020). There is significant evidence that the LCFA erroneously breaks up very large,
158   long-duration stratiform lightning flashes ("megaflashes"; Peterson 2019, 2021b), mainly due to

159 computational optimizations that improve realtime latency. This issue leads to the identification
160 of multiple flashes when in reality there was only a single megaflash. However, because such
161 flashes are rare (< 1% of the GLM dataset), they should not influence the results of this study.
162
163 2.2 Lightning Mapping Array (LMA)
164
165 The RELAMPAGO LMA was deployed during November 2018 through April 2019; i.e.,
166 the austral warm season. The centroid of the LMA was near the city of Córdoba, Argentina.
167 LMAs map lightning in 3D using Global Positioning System (GPS) time-of-arrival techniques
168 (Rison et al. 1999), and are generally considered to detect nearly all lightning within relatively
169 close range of network center (e.g., Thomas et al. 2004). The network consisted of up to 11
170 stations during this time; however, the number of stations operating on a given day was variable.
171 Generally at least 7 stations were operational, and more typically 9+. The published
172 RELAMPAGO LMA Level-2 dataset was used in this study (Lang 2020). This dataset consists
173 of individual VHF source locations as well as identified flashes using the processing approach by
174 Lang et al. (2020). The main constraints on the flash identification were a maximum of 150 ms
175 and 3 km between successive sources in a flash, and a flash could have a 3-s maximum duration.
176 LMA flashes were defined using thee different minimum thresholds – 3, 10, and 100 points – in
177 order to explore the impact of smaller vs. larger flashes on GLM DE. Because the LMA was still
178 being installed and improved during significant portions of November, this study focused on the
179 December-April period.
180
181 2.3 Analysis Methodology
182
183 This study focused only on lightning within 100 km of the RELAMPAGO LMA
184 centroid, as Lang et al. (2020) found that LMA performance was optimized within this region.
185 This occurred on 61 thunderstorm case days during December-April deployment (i.e., one or
186 more thunderstorms occurred roughly every other day). There were additional days with only 1-2
187 LMA flashes (1 January, 2 and 25 February) that were excluded from this total. Though 26
188 December had LMA lightning, GLM observations were missing for the relevant time period, so
189 this day also was excluded from analysis.
190 For the statistical validation, the main time unit for determining flash rates was 10
191 minutes. Besides being conveniently equal to the 10-minute data files provided by the LMA
192 processing algorithm (Lang 2020), this also reduced noise and focused on broad-based flash and
193 instrument performance trends within the 100-km radius domain. A GLM flash matched an
194 LMA flash if its centroid occurred within 500 ms and 25 km of at least one LMA flash. Due to
195 the fundamentally different nature of the GLM (optical) and LMA (VHF) measurements, as well
196 as the coarser ~10-km resolution of GLM, a GLM flash was allowed to match multiple LMA
197 flashes if the time and distance criteria above were all met. This benefitted GLM DE even if
198 GLM flash rates in the domain were well below LMA flash rates. Sensitivity studies were
199 performed with these spatiotemporal matching criteria halved (250 ms and 12.5 km) and doubled
200 (1000 ms and 50 km). GLM flashes were initially restricted to 150 km of LMA centroid before
201 performing any spatiotemporal matching. This allowed GLM flashes just outside the 100-km
202 radius of analysis to match with LMA flashes inside the radius.
203 Day (1100-2200 UTC) and Night (0000-0830 UTC) were broken out, with transition
204 periods (2200-0000 and 0830-1100 UTC) only included in Overall statistics. The transition

205 periods were made wide enough to exclude any seasonal changes in sunrise/sunset during
206 December-April. For example, around austral summer solstice daytime is longer than 1100-2200
207 UTC, but this is not true after the austral autumnal equinox.
208   Sensitivity studies were done that examined the possible benefits of improved GLM (or
209 GLM-like) DE of missed flashes. This simulated the impacts of 0-100% improvement in the
210 identification of missed LMA flashes by a spaceborne sensor; that is, an improved sensor or
211 algorithm that was able to resolve (and thus match) additional individual small LMA flashes.
212 This could include flashes that were fully missed by GLM, as well as more than one of the
213 multiple LMA flashes that were allowed to match a single GLM flash. In the latter case, this
214 simulated an improved ability by a spaceborne instrument to resolve these individual small, weak
215 flashes that are captured by the LMA without amalgamating them into a single, lower-resolution
216 optical flash seen by GLM. For the above analysis, 1-minute flash rates within 100-km of the
217 LMA were calculated for both GLM and the LMA on all case days analyzed for the statistical
218 DE study (which was done at 10-minute resolution, see above).
219   Lightning jumps (LJs) were defined following the methodology of Chronis et al. (2015).
220 Similar to that study, the average 2-minute flash rate of the most recent 14 minutes of lightning
221 was computed, and then the standard deviation of 2-minute flash rates were computed for the
222 most recent 12 minutes. The most recent 2-minute flash rate was then compared to the average,
223 and if it was greater than 3 times the standard deviation above the average, and the flash rate was
224 greater than 25 min^{-1}, then an LJ was identified. Chronis et al. (2015) explored a variety of α
225 (multiplicand of the standard deviation, σ) and absolute flash rate thresholds, and found that LJs
226 correspond to significant kinematic and microphysical changes in a thunderstorm. Analysis by
227 Schultz et al. (2015, 2017) also supported this inference. The present study used α of 3 and the
228 25 min^{-1} threshold to limit the focus to the strongest LJs, those that were most likely to truly
229 correspond to significant thunderstorm evolution, as opposed to potential noise. After an LJ was
230 identified, 10 minutes were required to pass before another LJ could be identified.
231   LJs for both the LMA and GLM were computed, with GLM LJs recomputed according to
232 0-100% improvements in DE as described above. A limitation of this analysis, compared to
233 Chronis et al. (2015) and Schultz et al. (2015, 2017), was that individual thunderstorms were not
234 isolated and tracked. All storms within 100 km were allowed to contribute to the LJ analysis.
235 This is another reason this study only focused on stronger LJs, to limit the effect of a mixture of
236 evolutionary states within multicellular storms on the statistics. In addition, this study did not
237 consider a storm's propensity to produce severe weather relative to an LJ; the focus was solely
238 on significant thunderstorm evolutionary changes within the analysis domain, as indicated by the
239 presence of an LJ.
240   False alarm rates were not explored in this study, as that would have required also
241 analyzing non-thunderstorm time periods. As discussed earlier, false alarms are a known issue
242 with GLM, but this study was primarily focused on DE as a function of flash rate and
243 flash/thunderstorm behavior. In addition, significant progress has been made on reducing false
244 alarms and artifacts in GLM-16 since 2018-2019 (e.g., Bateman et al. 2021), while reduced DE

245 during thunderstorm intensification or anomalous periods remains an issue where limited
246 progress has been made (e.g., Rutledge et al. 2020).
247
248 **3 Results**
249
250   3.1 Overview
251
252   Figure 1 shows an example set of time series exemplifying GLM performance during
253 RELAMPAGO, which helps to motivate this study. Similar figures for other cases can be found
254 in Lang et al. (2020). The case in question here is 23 February 2019, where an intense
255 thunderstorm transited through the southern portion of the LMA domain. Initially, GLM DE was
256 nearly 100% as LMA flash rate was low and flashes tended to have a large (~100 or more)
257 number of points. However, as the storm intensified flashes grew smaller (i.e., fewer points per
258 flash), and LMA flash rates reached a peak of ~80 min^{-1} (averaged over a 10-minute period) at
259 two separate times (during the 0400 and 0500 UTC hours, respectively). Flash rates then
260 weakened (to ~40 min^{-1}) before the storm exited the analysis domain. While GLM was broadly
261 correlated with the LMA, in that it also showed an enhancement and then a reduction in
262 lightning, GLM peak flash rates were more than a factor of 4 lower. This was primarily due to a
263 very large reduction in GLM DE when the thunderstorm intensified, down to less than 20%
264 during part of 0500-0600 UTC. This hour-long time period also corresponded to when the storm
265 appeared to be anomalously electrified, according to Medina et al. (2021); mean source altitude
266 also decreased during this time period. Moreover, due to some complexities in the GLM DE
267 curves, where 100+ point flash DE remained high into the 0400 UTC hour before finally
268 collapsing like the 10+ point DE did an hour earlier, GLM appeared to identify an earlier time
269 period than the LMA as the flash rate maximum (roughly 30 minutes earlier, in fact). In addition,
270 GLM did not resolve the second LMA peak during 0520-0530 UTC.
271   These single-case results illustrate the major themes of this study. For example, GLM can
272 have high DE (particularly for larger flashes), but when storms are intensifying DE appears to be
273 anticorrelated with actual flash rate. GLM DE also appears to be negatively impacted by
274 transient anomalous periods in thunderstorms. Ultimately, this makes GLM's response in intense
275 and/or anomalous storms much more muted than it ideally should be, limiting the utility of GLM
276 flash rate to identify intense storms (e.g., Murphy & Said 2020).
277   The remainder of this Results section will build on this case study, as well as the work of
278 Lang et al. (2020), to explore these themes in much more quantitative and statistical detail. In

279 addition, the effects of potential improvements in spaceborne optical lightning DE will be
280 explored.
281
282
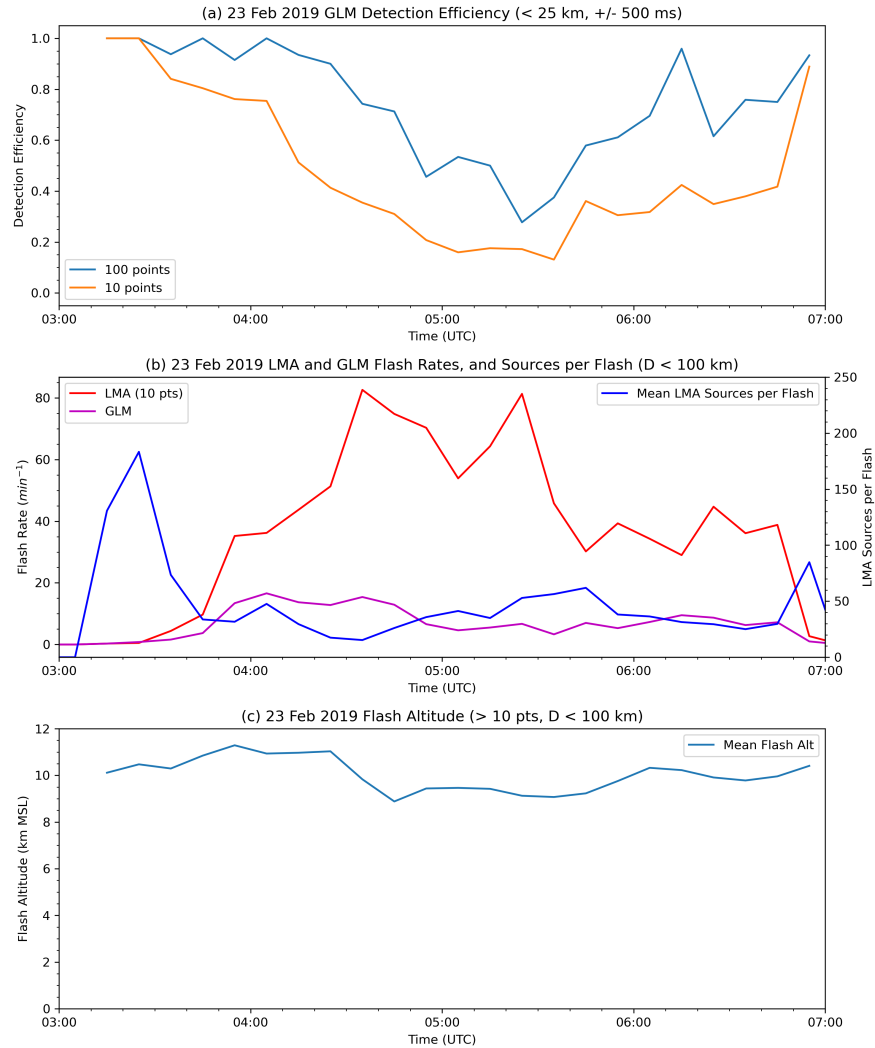
283
Figure 1. GLM and LMA observations within 100 km of the LMA on 23 February 2019. (a)
Time series of GLM DE for LMA-identified flashes with 10+ and 100+ points. (b) LMA and
GLM flash rates, and mean LMA sources per flash. (c) Mean LMA flash altitude.
287

288   3.2 Statistical Analysis of GLM Detection Efficiency
289

290   Between all 61 case days, there were 8762 possible ten-minute periods to enable DE and
291 correlation analyses. Depending on which flash rate was computed (e.g., GLM vs. LMA, 3-point
292 vs. 100-point), the actual number of ten-minute periods with lightning ranged within 2105-2502.
293 Correlations were done assuming these periods with lightning were linked as a continuous time
294 series. This is justified as flash rates nearly always tapered toward 0 near the start and end of

295   individual cases with lightning. Spearman correlations were computed as these do not assume a
296   linear relationship between the variables, only a monotonic one.

297   Statistics from the analysis are presented in Table 1. Results are broken out by the
298   standard 25-km and 500-ms matching criteria as well as whether those criteria were halved or
299   doubled. Day, Night, and Overall statistics are also provided. Discussion of this Table will focus
300   on the broader trends. Overall, for a 10-point minimum threshold to define an LMA flash, GLM
301   detected ~75% of LMA lightning, which met GLM's performance requirements (Goodman et al.
302   2013). Decreasing the threshold to 3-points only hurt DE by 1-5%. Increasing the threshold to
303   100 points improved DE by ~10-20%. Halving the matching criteria reduced DE by ~10-20%
304   (which reduced GLM well below 70% DE except for 100+ point flashes), while doubling the
305   criteria improved DE by ~5-10%. As expected, GLM performance during daytime was
306   significantly less than nighttime, again ~10-20% worse. GLM DE at night could exceed 90%,
307   depending on matching criteria and LMA points threshold. Overall, the statistics indicated very
308   good overall DE performance by GLM, but this performance was sensitive to specific thresholds
309   used in the analysis.

310   Medina et al. (2021) identified 38 hourlong blocks (their unit of analysis) during
311   December 2018 through April 2019 when the LMA indicated anomalous lightning behavior.
312   This behavior was determined by the use of an automated charge identification algorithm, called
313   Chargepol, which estimated the polarity, altitude, and vertical depth of charge layers based on
314   bulk flash behavior. Within these 38 hourlong blocks, there were 209 total ten-minute periods
315   with LMA lightning (this was roughly 8-10% of all lightning-producing periods during
316   December-April). Overall DE statistics for these anomalous periods are presented in Table 1.
317   The DE statistics were not further broken down into Day vs. Night due to the reduced sample
318   size. Under the standard matching criteria, for 10+ point LMA flashes DE was reduced to ~51%.
319   This DE was again sensitive to matching criteria and LMA points threshold, but overall ~20-
320   25% decreases in DE were common during anomalous scenarios.

321   Moving to the Spearman correlations, under the standard criteria (25-km, 500-ms, 10+
322   points) GLM and LMA flash rates were highly correlated ($r = 0.95$), and this was largely
323   insensitive to Day vs. Night, as well as halving or doubling of the spatiotemporal matching
324   criteria (0.95-0.97 range). Somewhat counterintuitively (since it improved GLM DE), increasing
325   the LMA points threshold to 100 actually reduced the flash rate correlation, to a range of 0.85-
326   0.89. However, increasing the point threshold that high actually reduced the overall population of
327   LMA flashes by ~70%. In that scenario, the assumptions underpinning the correlation analysis
328   (that flash rates tapered toward zero only near the beginning and end of a given lightning case)
329   became less well-supported. As many studies have noted, flashes tend to become smaller as a
330   thunderstorm intensifies. Thus, the relative fraction of 100+ point flashes should decrease when
331   that occurs, which should act to decorrelate the LMA and GLM time series. This decorrelation
332   trend when using the 100-point threshold can be seen elsewhere in Table 1 as well.

333   Despite the robustly high correlation between GLM and LMA flash rates, GLM DE was
334   actually significantly anticorrelated with LMA flash rate. The baseline correlation under the
335   aforementioned standard criteria was -0.49, and this was largely insensitive to halving or
336   doubling the spatiotemporal matching criteria, as well as the LMA points threshold (the range
337   was -0.41 to -0.50). What appeared to impact the degree of anticorrelation was Day vs. Night,

338 with nighttime anticorrelations larger than daytime. The already-reduced GLM DE during
339 daytime appeared to be playing a role in this difference.
340
341 **Table 1.** GLM detection efficiencies and Spearman correlation coefficients vs. the
342 RELAMPAGO LMA under various scenarios. *Correlation not significant at 99% confidence
343 level.

	25 km and 500 ms			12.5 km and 250 ms			50 km and 1 s		
	Day	**Night**	**Overall**	**Day**	**Night**	**Overall**	**Day**	**Night**	**Overall**
GLM DE		*%*			*%*			*%*	
3+ pts/flash	67.2	82.4	73.5	51.0	60.6	54.6	75.7	91.9	82.9
10+ pts/flash	68.1	83.6	74.6	54.3	64.6	58.2	75.9	92.3	83.2
100+ pts/flash	81.2	91.6	85.2	69.2	76.2	71.4	86.1	96.9	90.5
Anomalous GLM DE									
3+ pts/flash			50.6			33.9			63.2
10+ pts/flash			50.9			35.9			63.1
100+ pts/flash			69.1			54.8			77.2
GLM rate vs. LMA rate		*Spearman Correlation*			*Spearman Correlation*			*Spearman Correlation*	
3+ pts/flash	0.95	0.97	0.95	0.95	0.97	0.96	0.95	0.97	0.96
10+ pts/flash	0.95	0.97	0.95	0.95	0.97	0.95	0.95	0.97	0.95
100+ pts/flash	0.85	0.89	0.85	0.85	0.89	0.85	0.85	0.89	0.85
GLM DE vs. LMA rate									
3+ pts/flash	-0.37	-0.61	-0.50	-0.43	-0.49	-0.47	-0.28	-0.52	-0.41
10+ pts/flash	-0.37	-0.60	-0.49	-0.41	-0.46	-0.45	-0.28	-0.53	-0.42
100+ pts/flash	-0.43	-0.58	-0.49	-0.42	-0.42	-0.41	-0.39	-0.57	-0.47
GLM DE vs. LMA altitude									
3+ pts/flash	-0.35	-0.34	-0.34	-0.27	-0.23	-0.25	-0.30	-0.27	-0.29
10+ pts/flash	-0.23	-0.30	-0.24	-0.20	-0.20	-0.18	-0.18	-0.23	-0.19
100+ pts/flash	-0.04*	-0.10	-0.06	-0.06*	-0.10	-0.08	0.02*	-0.06*	-0.01*
GLM DE vs. LMA pts/flash	0.40	0.18	0.27	0.46	0.30	0.37	0.30	0.05*	0.15

344
345   GLM DE vs. mean LMA flash altitude was anticorrelated (standard result was -0.24),
346 which is somewhat counterintuitive since previously a reduction of DE during anomalous
347 periods was noted. This was likely due to competing trends, which ultimately summed to a
348 weakly negative overall correlation. Certainly, anomalous periods tend to be associated with
349 lower flash altitudes. However, as Lang et al. (2020) and others have noted, flash altitude can
350 increase during thunderstorm intensification, and as Table 1 shows GLM DE was anticorrelated
351 with LMA flash rate. Finally, larger flashes tended to be more readily detected by GLM, and
352 these flashes are often associated with more stratiform lightning, which often is lower in altitude
353 than lightning contained within deep convection. The influence of these competing trends may
354 also be seen in the increased sensitivity to various matching criteria and points thresholds, where
355 the anticorrelation can range from statistical insignificance to as high as -0.35.
356   The last row in Table 1 concerns GLM DE vs. mean points per LMA flash. Here, data for
357 3+ point flashes (i.e., the largest LMA flash dataset used in this study) were examined. The
358 standard correlation was 0.27, and this was highly sensitive (range of 0.05-0.46) to the choice of
359 criteria. In general, criteria that tended to reduce baseline GLM DE (e.g., focusing on Day,

360 halving spatiotemporal criteria, etc.) usually improved this correlation, while criteria that tended
361 to increase DE (e.g., Night, doubling) reduced the correlation, sometimes to the point of
362 statistical insignificance. Thus, the occurrence of larger flashes (i.e., those with more LMA
363 points) tended to improve DE at the margins, when GLM DE was already being throttled by
364 other restrictions. For example, since nighttime GLM DE during RELAMPAGO was already
365 high to begin with, making flashes a little bit bigger didn't have as strong an effect as during the
366 daytime. This trend is also visible in Table 1's GLM DE entries, where (for example) DE
367 improvements from 10- to 100-point thresholds were greater during Day than Night.
368
369   3.3 Investigation of the Impact of Improved GLM Detection Efficiency
370
371   As has been demonstrated, GLM DE was significantly anticorrelated with LMA flash
372 rate during RELAMPAGO (Table 1). In addition, the ratio of LMA flashes to GLM flashes
373 seemed to grow larger as flash rate increased (e.g., Fig. 1). Recall that because the flash
374 matching process allowed a single GLM flash to correspond to more than one LMA flash, the
375 absolute ratio of LMA flashes to GLM flashes could be large even if GLM DE was high. For the
376 entire December-April time period, the ratio of LMA flashes to GLM flashes was 2.9:1 (10+
377 points/flash). The behavior of this ratio as a function of 10-minute-average LMA flash rates is
378 shown in Fig. 2. As can be seen, the ratio increased approximately monotonically with LMA
379 flash rate (Fig. 2a), up to a 10-minute rate of 250 min^{-1}, though the relationship grew noisier as
380 sample size declined at higher flash rates (Fig. 2b). This reflected the mutually reinforcing
381 effects of reduced GLM DE at high flash rates, as well as an increased probability that a single
382 GLM flash would match with more than one LMA flash when LMA rates were high.
383   The net effect is that GLM response becomes increasingly dampened as LMA flash rates
384 increase to very high values. GLM rate of increase is throttled as storms intensify, as are the
385 absolute flash rates (Fig. 1; Lang et al. 2020). This would be expected to decorrelate GLM and
386 LMA during peak storm intensities, and also could affect the identification of LJs within GLM
387 data.
388   As discussed in the Introduction, this issue should also affect other spaceborne optical
389 lightning mappers that share common design characteristics with GLM (e.g., OTD, TRMM/ISS
390 LIS, FORTE, LMI, and MTG-LI). The exact details of how this manifests in their respective
391 datasets will vary based on specific instrument and algorithm characteristics, but all of these
392 sensors are/were likely vulnerable to undercounting flashes relative to an LMA during the
393 intense (or anomalous) portions of thunderstorm lifecycles (e.g., Zhang and Cummins 2020).
394 Thus, it is useful to explore the expected impacts of a future spaceborne sensor (or future

395 algorithm improvements to an existing sensor), which could be better designed to address this
396 shortcoming.
397
398
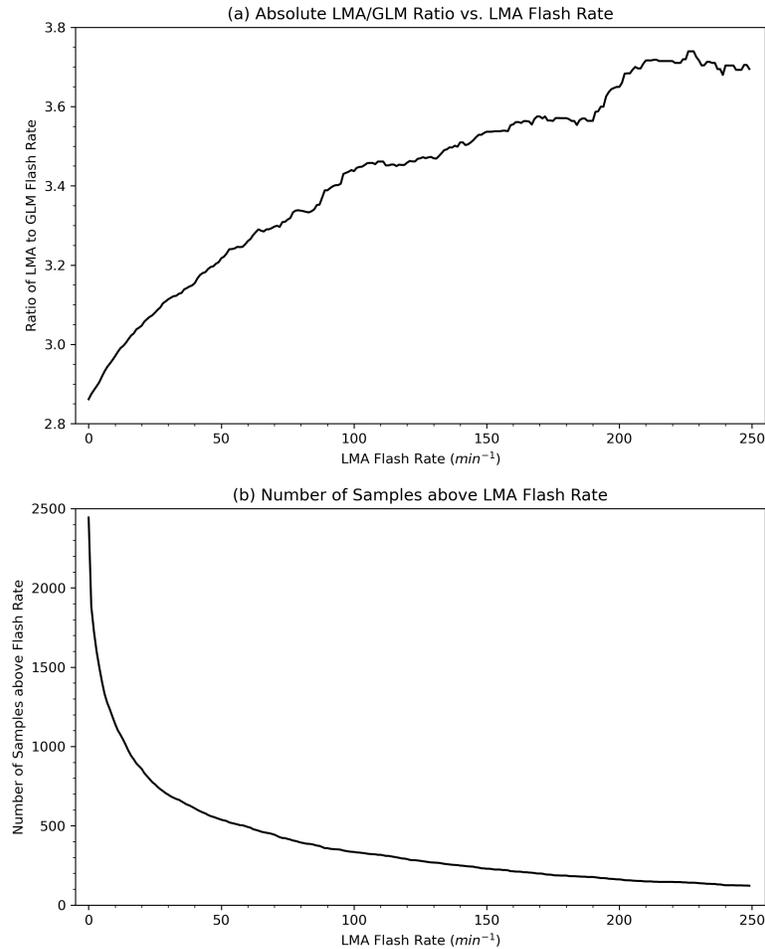
399
400 **Figure 2.** (a) Ratio of LMA to GLM flash rates, as a function of LMA flash rate. (b) Number of
401 samples informing the time series in (a) as a function of LMA flash rate.
402
403   The improvements could be accomplished in a number of ways (e.g., more sensitive
404 optics, additional complementary sensors/channels, improved spatiotemporal resolution, more
405 optimized processing algorithms, etc.), but the present study is simply focused on aggregate
406 improvements in flash detection capability, which can mean both increased DE as well as
407 improved ability to distinguish between separate small flashes. For this analysis the focus will be
408 on 0-100% improvements (in 10% bins) in flash identification relative to the LMA baseline. That

409   is, in a given minute, LMA flash rate will be *x*, GLM flash rate will be *y*, where *y* < *x* and an
410   "improved GLM" flash rate will be indicated as

412    $$y' = y + a\,(x - y),$$

414   where *y′* is the improved flash rate and *a* is the fractional improvement in flash detection
415   capability (range 0.0-1.0, in 0.1 steps, as mentioned above).
416   Figure 3 shows an example of how this manifested during the 23 February 2019 case also
417   studied in Fig. 1. The LMA time series (Fig. 3a) shows multiple intensifying and decay stages,
418   and the LJ methodology identified a total of 6 jumps. The unimproved GLM time series (Fig. 3b)
419   is significantly attenuated relative to the LMA, and flash rates and rate increases are too small to
420   identify any LJs. However, a 30% improvement in flash detection capability (Fig. 3c) would
421   bring the GLM closer in line with the LMA, and would reveal at least 3 LJs relatively close in
422   time to the respective LMA-identified LJs. Though fundamental issues still persist even with
423   these increased flash detections, there are demonstrable quantitative improvements in the ability
424   for the spaceborne instrument to characterize thunderstorms.
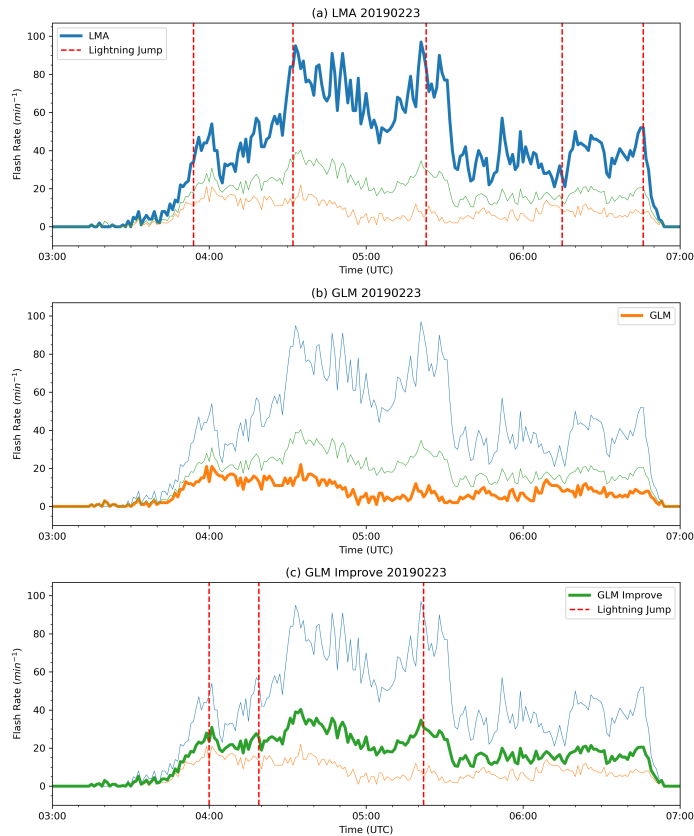
Figure 3. One-minute LMA, GLM, and improved GLM (assuming 30% increase in flash
detectability relative to the LMA) for 23 February 2019. (a) Focused on LMA, with associated
detected LJs. (b) focused on GLM, with no detected LJs. (c) Focused on improved GLM, with
associated detected LJs.

432   Figure 4 shows the results for the entire December-April RELAMPAGO period, for 0-
433   100% improvements in flash detection capability. The flash rate Spearman correlations (Fig. 4a)

13

434 increase rapidly, from ~0.84 to ~0.94, with only a modest 20% improvement in flash detection
435 capability. Beyond 20%, the rate of improvement starts to decline as correlations asymptotically
436 approach 1.0. Note that initial correlations with 0% improvement are below the values seen in
437 Table 1, as the Fig. 4 analysis is based on 1-minute flash rates, not 10-minute rates. Unlike the
438 asymptotic behavior in Fig. 4a, the ratio of "improved GLM" LJs to LMA-identified LJs
439 responds approximately linearly to increased flash detection capability (Fig. 4b), though there is
440 evidence of transient diminishing returns between 10 and 20%, before returning to a steeper rate
441 of improvement within 20-100%. But overall, modest improvements in detectability lead to only
442 modest gains. For example, a 20% improvement in flash detectability only nets a ~10%
443 improvement in LJ detection (from the baseline ~50%). Meanwhile, to correctly identify 80% of
444 LMA LJs, an improved GLM (or GLM-like sensor) would have to detect a whopping 50% more
445 flashes.
446
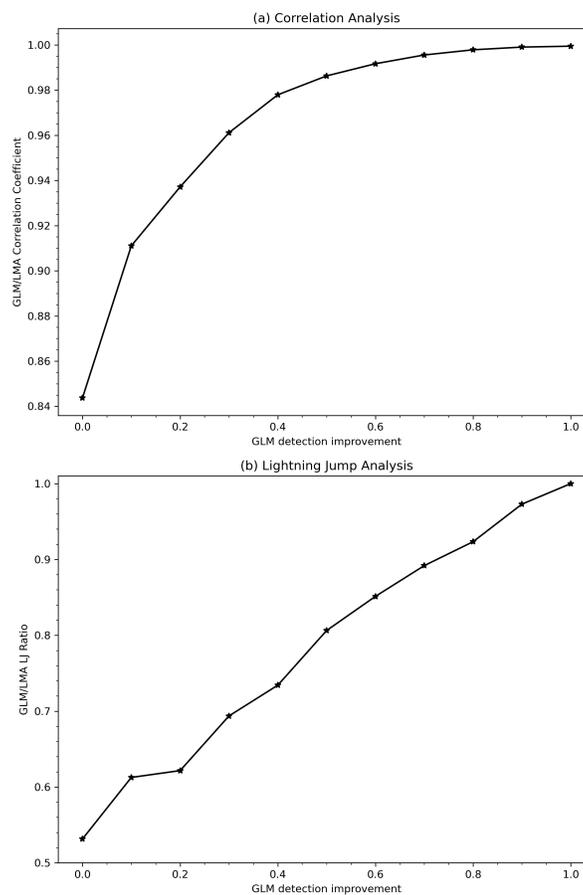
447
448 **Figure 4.** (a) Spearman correlations of 1-minute GLM vs. LMA flash rates, as a function of
449 GLM detectability improvement, for December 2018 through April 2019. (b) Ratio of the total
450 number of GLM- to LMA-detected LJs, as a function of GLM detectability improvement, for the
451 same period.
452
453 **4 Discussion and Conclusions**
454
455   This study focused on validation of the GLM-16 sensor using data from an LMA
456 deployed in north-central Argentina during 2018-2019, with special attention paid to DE as a

457 function of thunderstorm and lightning behavior. The analysis was confined to within 100 km of
458 the LMA centroid, where performance of the ground-based network was maximized (Lang et al.
459 2020). While GLM DE was high overall (~75%), and GLM and LMA flash rates were highly
460 correlated ($r \sim 0.95$), DE could vary significantly as thunderstorms evolved. In particular, GLM
461 DE was negatively correlated ($r \sim -0.5$) with LMA flash rate; that is, as LMA flash rates
462 increased within a thunderstorm, it became increasingly difficult for GLM to detect the
463 additional lightning. GLM DE was significantly better (~10-20%) during the nighttime vs
464 daytime, and for larger flashes vs. smaller (also ~10-20%). GLM DE was weakly correlated ($r \sim$
465 0.25) with the average number of points in LMA flashes, and this correlation was strongest in
466 situations where GLM DE otherwise had negative influences (e.g., daytime). Periods of
467 anomalous lightning (i.e., lightning associated with positively charged thunderstorm mid-levels,
468 loosely defined) were associated with DE reductions of ~20-25%. GLM DE was weakly
469 negatively correlated with flash altitude ($r \sim -0.25$), but this was very sensitive to spatiotemporal
470 matching criteria and LMA points thresholds for flashes, which suggested the influence of
471 multiple competing trends like anomalous lightning (worse expected DE), lower-altitude but
472 larger stratiform lightning (better expected DE), and flash altitude increasing with thunderstorm
473 intensification in normal-polarity storms (worse expected DE).
474   The overall high GLM DE occurred because this study allowed multiple LMA flashes to
475 match to a single GLM flash. While this was a reasonable accommodation given the
476 fundamentally different measurement technologies (one VHF- and ground-based, and capable of
477 geolocation within 10s of meters, while the other spaceborne and optical with geolocation ~10
478 km), in reality LMA flashes outnumbered GLM flashes by about a factor of 3, and this ratio
479 grew larger as LMA flash rate increased.
480   A sensitivity study was performed to examine the potential benefits of improved
481 spaceborne detectability of these small flashes that are so ubiquitous in intense convection as
482 measured by VHF sensors (e.g., Williams et al. 1999, Lang et al. 2000, Bruning and MacGorman
483 2013) as well as human-observed thunderstorms. In this context, detectability meant either
484 improved flash DE or improved ability to distinguish between individual small flashes.
485 Correlations improved significantly within the first 10-20% improvement in detectability, with
486 more asymptotic behavior afterward. Meanwhile, the ability to identify LJs within the convection
487 responded linearly to improved detectability. Overall, this suggests that sensor and/or
488 algorithmic improvements that achieve modest improvements (~10-20%) in flash detectability
489 could have a significant benefit for characterizing intense convection, but thereafter marginal
490 improvements in detectability would have to be increasingly weighed against the costs associated
491 with achieving that extra performance.
492   With spaceborne sensors that are always highly constrained by size, weight, and power
493 requirements, a 10-20% increase in performance in the future as technology improves could be a
494 reasonable goal. However, pushing beyond that likely would start to incur significant costs,
495 which this study finds might only provide additional modest benefits, suggesting that the
496 community involved in scientific analysis of intense/severe convection ought to consider other
497 options as well. That is, simply focusing on improving flash rate measurements to better match
498 those provided by LMAs will only provide diminishing returns relative to the expected costs
499 associated with achieving that goal from spaceborne platforms. Improving the spaceborne
500 technology is important, but improved algorithmic developments to better identify and
501 characterize intense/severe convection using lightning observations are also needed (i.e., simply
502 focusing on flash rates and identifying LJs is insufficient, from the spaceborne perspective).

503   Thankfully, there are a number of viable pathways to consider. Studies have found that
504   minimum and mean flash areas, as measured by spaceborne sensors like GLM, could provide
505   useful information about intensifying thunderstorms (e.g., Bruning et al. 2019). In addition,
506   group rate could provide information, since groups are a processing step removed from flashes in
507   GLM and related algorithms (Mach et al. 2007, Mach 2020), so analysis at that lower data level
508   reduces complexity. However, lightning group analysis needs to consider the presence (or lack
509   thereof) of stratiform lightning, which typically is associated with low flash rates but increased
510   group rates per flash (Peterson 2019). But more specifically, this study (in the context of many
511   others with similar results; e.g., Marchand et al. 2019) is a challenge to the lightning community
512   to develop algorithms that rely on more than just flash rates to characterize significant milestones
513   or processes in thunderstorm evolution, particularly when working with spaceborne lightning
514   observations.
515   This study has also demonstrated an innate 20-25% DE reduction with GLM when
516   anomalous lightning is occurring. This is consistent with related studies (e.g., Marchand et al.
517   2019, Murphy & Said 2020, Rutledge et a. 2020), and is on top of any additional DE reductions
518   associated with high flash rates. That is, an intense/severe anomalous storm with very high flash
519   rates could easily result in 20-30% DE for a spaceborne sensor like GLM (e.g., Fig. 1). This
520   result strongly argues for a spaceborne capability to measure lightning flash altitude, particularly
521   to identify the presence of anomalous storms. Indeed, the overall global frequency of anomalous
522   storms is poorly understood, even though it is highly likely that certain regions (e.g., Colorado
523   and similar climatological regimes) are disproportionately prone to their occurrence (e.g., Fuchs
524   et al. 2015). Lightning altitude may also play a role in terrestrial gamma-ray flash (TGF)
525   production (or at least detection of TGFs from space; e.g., Lopez et al. 2019) as well as the
526   production of transient luminous events (TLEs) such as sprites (e.g., Hu et al. 2002). One
527   potential option for this has been studies like Peterson et al. (2021), who used combined optical
528   and VHF measurements to measure lightning flash altitude from space.
529   The ability to resolve the vertical distribution of lightning from space (including
530   retrievals of lightning channel length; Koshak et al. 2014) also would greatly benefit studies of
531   lightning-produced nitrogen oxides (LNOx). LNOx, along with lightning-produced hydroxyl
532   radicals (OH), has important implications for the Earth's climate due to the species' strong
533   influence on the global lifecycles of tropospheric ozone and methane, which are powerful
534   greenhouse gases (Murray 2016, Wu et al. 2023).
535

Open Research

RELAMPAGO LMA data may be obtained from
http://dx.doi.org/10.5067/RELAMPAGO/LMA/DATA101. GLM Level-2 LCFA data may be obtained from https://doi.org/10.7289/V5KH0KK6. Analysis software used in this study was based on Python, and made used of major packages including numpy, scipy, matplotlib, pandas, xarray, h5py, and Jupyter, as well as more customized libraries like lmatools (https://github.com/deeplycloudy/lmatools). The specific analysis notebooks are undergoing the NASA open source release process and will be made available by formal publication in accordance with NASA Science Mission Directorate Policy Document 41a (https://science.nasa.gov/science-red/s3fs-public/atoms/files/SMD-information-policy-SPD-41a.pdf).

References

Bateman, M., & Mach, D. (2020). Preliminary detection efficiency and false alarm rate assessment of the Geostationary Lightning Mapper on the GOES-16 satellite. Journal of Applied Remote Sensing, 14(3), 032406-032406.

Bateman, M., Mach, D., & Stock, M. (2021). Further investigation into detection efficiency and false alarm rate for the geostationary lightning mappers aboard GOES-16 and GOES-17. Earth and Space Science, 8, e2020EA001237. https://doi.org/10.1029/2020EA001237

Blakeslee, R.J., Lang, T.J., Koshak, W.J., Buechler, D., Gatlin, P., Mach, D.M., Stano, G.T., Virts, K.S., Walker, T.D., Cecil, D.J., Ellett, W., Goodman, S.J., Harrison, S., Hawkins, D.L., Heumesser, M., Lin, H., Maskey, M., Schultz, C.J., Stewart, M., Bateman, M., Chanrion, O. and Christian, H. (2020), Three Years of the Lightning Imaging Sensor Onboard the International Space Station: Expanded Global Coverage and Enhanced Applications. J. Geophys. Res. Atmos., 125: e2020JD032918. https://doi.org/10.1029/2020JD032918

Bruning, E. C., and D. R. MacGorman, 2013: Theory and Observations of Controls on Lightning Flash Size Spectra. J. Atmos. Sci., 70, 4012–4029, https://doi.org/10.1175/JAS-D-12-0289.1.

582 Bruning, E., Tillier, C. E., Edgington, S. F., Rudlosky, S. D., Zajic, J., Gravelle, C., et al. (2019).
583 Meteorological imagery for the geostationary lightning mapper. Journal of Geophysical
584 Research: Atmospheres, 2019; 124: 14285– 14309. https://doi.org/10.1029/2019JD030874

586 Bruning, E. C., Weiss, S. A., & Calhoun, K. M. (2014). Continuous variability in thunderstorm
587 primary electrification and an evaluation of inverted-polarity terminology. Atmospheric
588 Research, 135, 274-284.

590 Cao, D.; Lu, F.; Zhang, X.; Yang, J. Lightning Activity Observed by the FengYun-4A Lightning
591 Mapping Imager. Remote Sens. 2021, 13, 3013. https://doi.org/10.3390/rs13153013

593 Chanrion, O., Neubert, T., Lundgaard Rasmussen, I. et al. The Modular Multispectral Imaging
594 Array (MMIA) of the ASIM Payload on the International Space Station. Space Sci Rev 215, 28
595 (2019). https://doi.org/10.1007/s11214-019-0593-y

597 Christian, H. J., et al., Global frequency and distribution of lightning as observed from space by
598 the Optical Transient Detector, J. Geophys. Res., 108(D1), 4005, doi:10.1029/2002JD002347,
599 2003.

601 Chronis, T., L. D. Carey, C. J. Schultz, E. V. Schultz, K. M. Calhoun, and S. J. Goodman, 2015:
602 Exploring Lightning Jump Characteristics. Wea. Forecasting, 30, 23–37,
603 https://doi.org/10.1175/WAF-D-14-00064.1.

605 Fuchs, B. R., Rutledge, S. A., Bruning, E. C., Pierce, J. R., Kodros, J. K., Lang, T. J.,
606 MacGorman, D. R., Krehbiel, P. R., and Rison, W. (2015), Environmental controls on storm
607 intensity and charge structure in multiple regions of the continental United States. J. Geophys.
608 Res. Atmos., 120, 6575– 6596. doi: 10.1002/2015JD023271.

610 GOES-R Algorithm Working Group and GOES-R Series Program (2018): NOAA GOES-R
611 Series Geostationary Lightning Mapper (GLM) Level 2 Lightning Detection: Events, Groups,
612 and Flashes. NOAA National Centers for Environmental Information. doi:10.7289/V5KH0KK6.

614 Gatlin, P. N., and Goodman S. J. , 2010: A total lightning trending algorithm to identify severe
615 thunderstorms. J. Atmos. Oceanic Technol., 27, 3–22, doi:10.1175/2009JTECHA1286.1.

617 Goodman, S. J., Blakeslee, R. J., Koshak, W. J., Mach, D., Bailey, J., Buechler, D., ... & Stano,
618 G. (2013). The GOES-R geostationary lightning mapper (GLM). Atmospheric research, 125, 34-
619 49.

621 Holmlund, K., and Coauthors, 2021: Meteosat Third Generation (MTG): Continuation and
622 Innovation of Observations from Geostationary Orbit. Bull. Amer. Meteor. Soc., 102, E990–
623 E1015, https://doi.org/10.1175/BAMS-D-19-0304.1.

625 Hu, W, Cummer, S., Lyons, W. A., and Nelson, T., Lightning charge moment changes for the
626 initiation of sprites, Geophys. Res. Lett., 29(8), doi:10.1029/2001GL014593, 2002.
627

628 Jacobson, A. R., & Light, T. E. L. (2012, February). Revisiting" Narrow Bipolar Event"
629 intracloud lightning using the FORTE satellite. In Annales geophysicae (Vol. 30, No. 2, pp. 389-
630 404). Göttingen, Germany: Copernicus Publications.

632 Koshak, W., Peterson, H., Biazar, A., Khan, M., & Wang, L. (2014). The NASA lightning
633 nitrogen oxides model (LNOM): Application to air quality modeling. Atmospheric Research,
634 135, 363-369.

636 Kummerow, C., W. Barnes, T. Kozu, J. Shiue, and J. Simpson, 1998: The Tropical Rainfall
637 Measuring Mission (TRMM) Sensor Package. J. Atmos. Oceanic Technol., 15, 809–817,
638 https://doi.org/10.1175/1520-0426(1998)015<0809:TTRMMT>2.0.CO;2.

640 Lang, Timothy, 2020. Remote sensing of Electrification, Lightning, And Mesoscale/microscale
641 Processes with Adaptive Ground Observations (RELAMPAGO) Lightning Mapping Array
642 (LMA). Dataset available online from the NASA Global Hydrometeorology Resource Center
643 DAAC, Huntsville, Alabama, U.S.A. DOI:
644 http://dx.doi.org/10.5067/RELAMPAGO/LMA/DATA101

646 Lang, T. J., & Bang, S. D. (2022). Exploring the scientific utility of combined spaceborne Lidar
647 and Lightning observations of thunderstorms. Earth and Space Science, 9, e2022EA002400.
648 https://doi.org/10.1029/2022EA002400

650 Lang, T. J., and Coauthors, 2020: The RELAMPAGO Lightning Mapping Array: Overview and
651 Initial Comparison with the Geostationary Lightning Mapper. J. Atmos. Oceanic Technol., 37,
652 1457–1475, https://doi.org/10.1175/JTECH-D-20-0005.1.

654 Lang, T. J., S. A. Rutledge, J. E. Dye, M. Venticinque, P. Laroche, and E. Defer, 2000:
655 Anomalously Low Negative Cloud-to-Ground Lightning Flash Rates in Intense Convective
656 Storms Observed during STERAO-A. Mon. Wea. Rev., 128, 160–173,
657 https://doi.org/10.1175/1520-0493(2000)128<0160:ALNCTG>2.0.CO;2.

659 López, J. A., Montanyà, J., van der Velde, O. A., Pineda, N., Salvador, A., Romero, D., et al.
660 (2019). Charge structure of two tropical thunderstorms in Colombia. Journal of Geophysical
661 Research: Atmospheres, 124, 5503– 5515. https://doi.org/10.1029/2018JD029188

663 Mach, D. M. (2020). Geostationary Lightning Mapper clustering algorithm stability. Journal of
664 Geophysical Research: Atmospheres, 125, e2019JD031900.
665 https://doi.org/10.1029/2019JD031900

667 Mach, D. M., Christian, H. J., Blakeslee, R. J., Boccippio, D. J., Goodman, S. J., and Boeck, W.
668 L. (2007), Performance assessment of the Optical Transient Detector and Lightning Imaging
669 Sensor, J. Geophys. Res., 112, D09210, doi:10.1029/2006JD007787.

671 Marchand, M., Hilburn, K., & Miller, S. D. (2019). Geostationary lightning mapper and Earth
672 networks lightning detection over the contiguous United States and dependence on flash

673 characteristics. Journal of Geophysical Research: Atmospheres, 124, 11552– 11567.
674 https://doi.org/10.1029/2019JD031039

676 Medina, B. L., Carey, L. D., Bitzer, P. M., Lang, T. J., & Deierling, W. (2022). The Relation of
677 environmental conditions with charge structure in central Argentina thunderstorms. Earth and
678 Space Science, 9, e2021EA002193. https://doi.org/10.1029/2021EA002193

680 Medina, B. L., Carey, L. D., Lang, T. J., Bitzer, P. M., Deierling, W., & Zhu, Y. (2021).
681 Characterizing charge structure in Central Argentina thunderstorms during RELAMPAGO
682 utilizing a new charge layer polarity identification method. Earth and Space Science, 8,
683 e2021EA001803. https://doi.org/10.1029/2021EA001803

685 Murphy, M. J., & Said, R. K. (2020). Comparisons of lightning rates and properties from the
686 U.S. National Lightning Detection Network (NLDN) and GLD360 with GOES-16 Geostationary
687 Lightning Mapper and Advanced Baseline Imager data. Journal of Geophysical Research:
688 Atmospheres, 125, e2019JD031172. https://doi.org/10.1029/2019JD031172

690 Murray, L.T. Lightning NO x and Impacts on Air Quality. Curr Pollution Rep 2, 115–133
691 (2016). https://doi.org/10.1007/s40726-016-0031-7

693 Nesbitt, S. W., and Coauthors, 2021: A Storm Safari in Subtropical South America: Proyecto
694 RELAMPAGO. Bull. Amer. Meteor. Soc., 102, E1621–E1644, https://doi.org/10.1175/BAMS-
695 D-20-0029.1.

697 Neubert, T., Østgaard, N., Reglero, V. et al. The ASIM Mission on the International Space
698 Station. Space Sci Rev 215, 26 (2019). https://doi.org/10.1007/s11214-019-0592-z

700 Peterson, M. (2019). Research applications for the Geostationary Lightning Mapper operational
701 lightning flash data product. Journal of Geophysical Research: Atmospheres, 124, 10205–
702 10231. https://doi.org/10.1029/2019JD031054

704 Peterson, M. (2020). Removing solar artifacts from Geostationary Lightning Mapper data to
705 document lightning extremes. Journal of applied remote sensing, 14(3), 032402-032402.

707 Peterson, M. (2021a). Holes in optical lightning flashes: Identifying poorly transmissive clouds
708 in lightning imager data. Earth and Space Science, 8, e2020EA001294.
709 https://doi.org/10.1029/2020EA001294

711 Peterson, M., 2021b: Where Are the Most Extraordinary Lightning Megaflashes in the
712 Americas?. Bull. Amer. Meteor. Soc., 102, E660–E671, https://doi.org/10.1175/BAMS-D-20-
713 0178.1.

715 Peterson, M., Light, T. E. L., & Shao, X.-M. (2021). Combined optical and radio-frequency
716 perspectives on a hybrid Cloud-to-Ground lightning flash observed by the FORTE satellite.
717 Journal of Geophysical Research: Atmospheres, 126, e2020JD034152.
718 https://doi.org/10.1029/2020JD034152

719

720 Quick, M. G., Christian, H. J., Virts, K. S., & Blakeslee, R. J. (2020). Airborne radiometric

721 validation of the geostationary lightning mapper using the Fly's Eye GLM Simulator. Journal of

722 Applied Remote Sensing, 14(4), 044518-044518.

723

724 Rison, W., Thomas, R. J., Krehbiel, P. R., Hamlin, T., and Harlin, J.: A GPS-based three-

725 dimensional lightning mapping system: Initial observations in central New Mexico, Geophys.

726 Res. Lett., 26, 3573–3576, https://doi.org/10.1029/1999GL010856, 1999.

727

728 Rudlosky, S. D., Goodman, S. J., Virts, K. S., & Bruning, E. C. (2019). Initial geostationary

729 lightning mapper observations. Geophysical Research Letters, 46, 1097– 1104.

730 https://doi.org/10.1029/2018GL081052

731

732 Rudlosky, S. D., and K. S. Virts, 2021: Dual Geostationary Lightning Mapper Observations.

733 Mon. Wea. Rev., 149, 979–998, https://doi.org/10.1175/MWR-D-20-0242.1.

734

735 Rust, W. D., MacGorman, D. R., Bruning, E. C., Weiss, S. A., Krehbiel, P. R., Thomas, R. J., ...

736 & Harlin, J. (2005). Inverted-polarity electrical structures in thunderstorms in the Severe

737 Thunderstorm Electrification and Precipitation Study (STEPS). Atmospheric Research, 76(1-4),

738 247-271.

739

740 Rutledge, S. A., Hilburn, K. A., Clayton, A., Fuchs, B., & Miller, S. D. (2020). Evaluating

741 Geostationary Lightning Mapper flash rates within intense convective storms. Journal of

742 Geophysical Research: Atmospheres, 125, e2020JD032827.

743 https://doi.org/10.1029/2020JD032827

744

745 Schultz, C. J., L. D. Carey, E. V. Schultz, and R. J. Blakeslee, 2015: Insight into the Kinematic

746 and Microphysical Processes that Control Lightning Jumps. Wea. Forecasting, 30, 1591–1621,

747 https://doi.org/10.1175/WAF-D-14-00147.1.

748

749 Schultz, C. J., L. D. Carey, E. V. Schultz, and R. J. Blakeslee, 2017: Kinematic and

750 Microphysical Significance of Lightning Jumps versus Nonjump Increases in Total Flash Rate.

751 Wea. Forecasting, 32, 275–288, https://doi.org/10.1175/WAF-D-15-0175.1.

752

753 Schultz, C. J., W. A. Petersen, and L. D. Carey, 2009: Preliminary Development and Evaluation

754 of Lightning Jump Algorithms for the Real-Time Detection of Severe Weather. J. Appl. Meteor.

755 Climatol., 48, 2543–2563, https://doi.org/10.1175/2009JAMC2237.1.

756

757 Soler, S., Gordillo-Vázquez, F. J., Pérez-Invernón, F. J., Luque, A., Li, D., Neubert, T., et al.

758 (2021). Global frequency and geographical distribution of nighttime streamer corona discharges

759 (BLUEs) in thunderclouds. Geophysical Research Letters, 48, e2021GL094657.

760 https://doi.org/10.1029/2021GL094657

761

762 Suszcynsky, D. M., Kirkland, M. W., Jacobson, A. R., Franz, R. C., Knox, S. O., Guillen, J. L.

763 L., and Green, J. L. (2000), FORTE observations of simultaneous VHF and optical emissions

from lightning: Basic phenomenology, J. Geophys. Res., 105(D2), 2191– 2201, doi:10.1029/1999JD900993.

Thomas, R. J., Krehbiel, P. R., Rison, W., Hunyady, S. J., Winn, W. P., Hamlin, T., and Harlin, J. (2004), Accuracy of the Lightning Mapping Array, J. Geophys. Res., 109, D14207, doi:10.1029/2004JD004549.

Virts, K. S., and W. J. Koshak, 2020: Mitigation of Geostationary Lightning Mapper Geolocation Errors. J. Atmos. Oceanic Technol., 37, 1725–1736, https://doi.org/10.1175/JTECH-D-19-0100.1.

Virts, K. S., and W. J. Koshak, 2023: Monte Carlo Simulations for Evaluating the Accuracy of Geostationary Lightning Mapper Detection Efficiency and False Alarm Rate Retrievals. J. Atmos. Oceanic Technol., 40, 219–235, https://doi.org/10.1175/JTECH-D-22-0050.1.

Wiens, K. C., S. A. Rutledge, and S. A. Tessendorf, 2005: The 29 June 2000 Supercell Observed during STEPS. Part II: Lightning and Charge Structure. J. Atmos. Sci., 62, 4151–4177, https://doi.org/10.1175/JAS3615.1.

Williams, E. R., and Coauthors, 1999: The behavior of total lightning activity in severe Florida thunderstorms. Atmos. Res., 51, 245–265, doi:10.1016/S0169-8095(99)00011-3.

Wu, Y., Pour-Biazar, A., Koshak, W. J., & Cheng, P. (2023). LNOx emission model for air quality and climate studies using satellite lightning mapper observations. Journal of Geophysical Research: Atmospheres, 128, e2022JD037406. https://doi.org/10.1029/2022JD037406

Zhang, D., & Cummins, K. L. (2020). Time evolution of satellite-based optical properties in lightning flashes, and its impact on GLM flash detection. Journal of Geophysical Research: Atmospheres, 125, e2019JD032024. https://doi.org/10.1029/2019JD032024